The Astrophysical Journal, 625:L79–L82, 2005 June 1

EMISSION-LINE SPECTROSCOPY OF DAMPED Lyα SYSTEMS: THE CASE OF SBS 1543+593/HS 1543+5921

Regina E. Schulte-Ladbeck,[1] Brigitte König,[1] Christopher J. Miller,[2] Andrew M. Hopkins,[1]
Igor O. Drozdovsky,[3] David A. Turnshek,[1] and Ulrich Hopp[4]
Received 2005 February 8; accepted 2005 April 25; published 2005 May 17

ABSTRACT

We report *HST*/STIS spectroscopy and Gemini/GMOS-N imaging of the Damped Lyα (DLA) system toward HS 1543+5921 caused by the host star-forming galaxy (SFG) SBS 1543+593. The Gemini image shows new morphological details of this well-resolved DLA galaxy. In combination with previous optical spectra, the new UV spectra enable us to compare, for the first time, ionized and neutral gas-phase α-element abundances derived from emission- and absorption-line spectroscopy, in a bona fide DLA galaxy. The abundances we determine using emission-line diagnostics agree with those from absorption-line diagnostics. We present our results on a metallicity versus redshift diagram that combines local H II regions and SFGs with high-redshift DLAs, and discuss implications for the chemical evolution of galaxies.

Subject headings: galaxies: abundances — galaxies: individual (SBS 1543+593) — quasars: absorption lines — quasars: individual (HS 1543+5921)

1. INTRODUCTION

Damped Lyα systems on the sight lines to background quasars exhibit high neutral hydrogen column densities and are thought to arise in early disk galaxies capable of sustaining star formation (Wolfe 1990). But over the last decade, only about a dozen DLA *galaxies* have been identified and imaged (e.g., Turnshek et al. 2002; Chen et al. 2005).

The chance projection of the galaxy SBS 1543+593 (z = 0.0096) and the background QSO HS 1543+5921 (z = 0.807) 2.″4 away from the center of the galaxy (Fig. 1) was discovered by Reimers & Hagen (1998). Bowen et al. (2001a, 2001b) noticed that the galaxy gives rise to a DLA system in the spectrum of the QSO. Schulte-Ladbeck et al. (2004) studied SBS 1543+593 using *Hubble Space Telescope* (*HST*) imaging and ground-based spectroscopy. They classified it an Sm dwarf galaxy with properties that are entirely in line with those of other local dwarf galaxies. Several of the 33 *HST*-discovered H II regions were analyzed with emission-line diagnostics. For the brightest region (No. 5), all emission lines necessary to derive the O and N abundances were detected.

SBS 1543+593 offers us an excellent opportunity to directly compare element abundances inferred from cool interstellar gas (DLAs) and ionized gas (SFGs). None of the previously imaged DLA galaxies resolve to show individual H II regions. In none of them does the sight line to the QSO intercept the disk of the galaxy well within its optical radius, let alone close to its center, thus eliminating concerns over metallicity gradients. SBS 1543+593 facilitates an important inquiry into the behavior of galaxy metallicities with redshift, because almost all available abundances at high redshifts are determined from QSO absorption-line studies and refer to iron-peak elements such as Zn and Cr (Pettini 2004), whereas at low redshifts, derivations of chemical abundances are based on nebular emission-line studies in star-forming regions and are primarily based on the α-capture element oxygen (e.g., Garnett 2004). Chen et al. (2005) recently derived O abundances from emission lines in one DLA and one sub-DLA galaxy; the QSOs' spectra allowed them to determine absorption-line abundances of Fe. These data are not suited to the comparison we are interested in here, because Fe is a highly depleted element; we do not know the α/Fe ratio, and their QSOs have impact parameters larger than the optical disks of the galaxies. SBS 1543+593 is unique, since it enables us to make a direct comparison between the emission- and absorption-line techniques, and allows us to contrast α-element abundances of a DLA and its host galaxy in a low-redshift QSO-galaxy pair.

2. OBSERVATIONS

Two sets of *HST*/Space Telescope Imaging Spectrograph (STIS) observations of the QSO HS 1543+5921 were performed (ID 9784, PI: D. Bowen) using grating G140M with a dispersion of 0.05 Å pixel^{-1} and centered at 1222.0 Å and on 1272.0 Å. We averaged the five exposures per configuration to one single spectrum in order to increase the signal-to-noise ratio.

The spectrum centered at 1222.0 Å covers the N I $\lambda\lambda$1199.5, 1200.2, 1200.7 triplet. The continuum is very noisy; and the lines are located in the blue wing of the Galactic Lyα line. For each line, we measure a lower and upper limit to its EW, by varying the continuum placement. This results in six EW values, each of which has a large uncertainty. The range of EWs will be translated into an abundance range below.

The spectrum centered at 1272.0 Å (see Fig. 2) is used to measure the individual lines of the S II triplet. The continuum level of S II (λ_{obs} = 1262.54 Å) is difficult to determine and therefore uncertain; we consider this measurement as a lower limit. S II (λ_{obs} = 1265.85 Å) is unblended, and the continuum level is well determined. S II (λ_{obs} = 1271.61 Å) is blended with a nearby Si II line. We used two Gaussian profiles to deblend the two lines. For an overview of the measured values, see Table 1.

We performed deep optical imaging using Gemini Multi-Object Spectrograph North (GMOS-N; see Fig. 1) equipped with the r_G0303 filter, a broadband filter (5620–6980 Å) with an effective wavelength of 6300 Å. A total of six dithered

[1] Department of Physics and Astronomy, University of Pittsburgh, 3941 O'Hara Street, Pittsburgh, PA 15260; rsl@phyast.pitt.edu, bkoenig@phyast.pitt.edu, ahopkins@anu.phyast.pitt.edu, turnshek@quasar.phyast.pitt.edu.
[2] Cerro Tololo Inter-American Observatory, Casilla 603, La Serena, Chile; cmiller@noao.edu.
[3] *Spitzer* Science Center, California Institute of Technology, MC 314-6, 1200 East California Boulevard, Pasadena, CA 91125; dio@ipac.calthech.edu.
[4] Universitätssternwarte München, Scheinerstrasse 1, D-81679 München, Germany; hopp@usm.uni-muenchen.de.

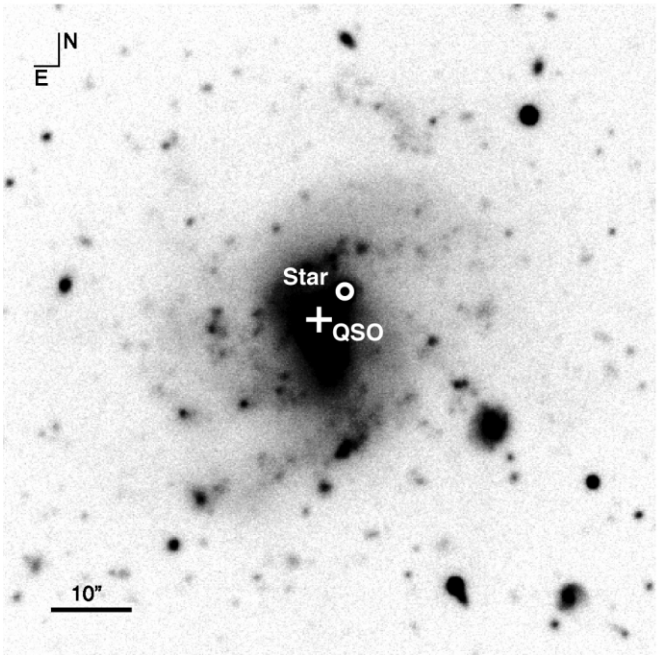

FIG. 1.—GMOS-N observations of SBS 1543+593 using the r_G0303 filter. To facilitate comparison with Fig. 1 of Schulte-Ladbeck et al. (2004), we marked the position of the QSO, which is located in the background of the galaxy, and a foreground star. Notice the extended spiral-arm system of the galaxy that is not visible on the *HST* images of Schulte-Ladbeck et al. (2004).

300 s exposures were taken. After pipeline calibration, the images were averaged to increase the signal-to-noise ratio.

The *HST* image published by Schulte-Ladbeck et al. (2004) showed only the inner saturated region of the new GMOS-N image. We now detect extended spiral arms with associated H II regions. Note also the two features to the northeast that are only revealed in this deep image. The image suggests a morphology that is still consistent with the previous classification of SBS 1543+593 as an Sm galaxy. Photometry of 193 regions within the image that are more extended than the stellar point-spread function was performed using the IRAF task DAOPHOT. Up to 140 could be H II regions, based on the fact that they lie within the disk of the galaxy. Spectroscopy is needed to confirm their nature and to measure their chemical abundances.

3. ABUNDANCE ANALYSIS: NEUTRAL GAS

The abundances of sulfur and nitrogen are derived using the measurements of the EWs and calculating the rest equivalent width (REW) using the redshift of the galaxy. Together with the oscillator strengths or *f*-values of Morton (1991), we derive column densities (N) from equation (8) of Petitjean (1998). This expression is only applicable to optically thin absorption lines on the linear part of the curve of growth. Table 1 shows that the equivalent widths of the three S lines used are in the same ratio as their *f*-values (within the errors), and therefore assuming the optically thin case appears to be valid. However, we must be concerned that the spectral resolution is insufficient to discern if there are any narrow saturated components contributing to the absorption lines. If such components are present, we may have underestimated the column density of S (but this would not invalidate the main result of the Letter).

In the following we will introduce a new nomenclature.[5] $[Y/X]_I$ refers to the element abundance of element Y with respect to element X in the neutral gas measured using absorption-line diagnostics, while $[Y/X]_{II}$ refers to it measured in H II regions by emission-line diagnostics.

[5] $[Y/X] = \log (Y/X) - \log (Y/X)_\odot$.

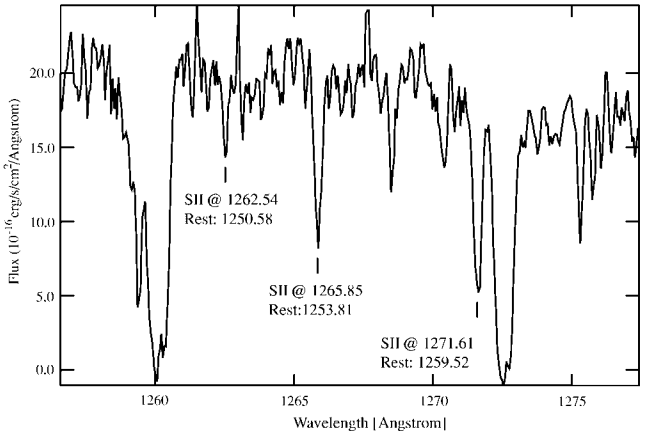

FIG. 2.—*HST*/STIS spectrum centered at 1272.0 Å showing the S II triplet. The spectrum was smoothed with a boxcar of 3 pixels.

Each of the six nitrogen REWs is converted to a column density. Considering the above-mentioned measurement uncertainties, we give a range of (0.12–1.80) × 10^{14} cm^{-2}, rather than a mean value for the column density. Consequently, we derive $-2.6 \lesssim [N/H]_I \lesssim -2.0$ and adopt the solar nitrogen abundance of 7.931 ± 0.111 from Holweger (2001).

We use a solar sulfur abundance of 7.20 (Grevesse & Sauval 1998). This is consistent with Prochaska et al. (2003b). Note that Holweger (2001) does not provide a sulfur abundance for the Sun. The REWs (λ = 1254 and 1259 Å) listed in Table 1 were used to calculate N(S II) = (1.10 ± 0.31) × 10^{15} cm^{-2} or $[S\,II/H]_I = -0.50 \pm 0.33$.

The ionization energies for sulfur are S I = 10.36 eV and S II = 23.33 eV. Abundance corrections in DLAs for ionization energies higher than $h\nu > 13.6$ eV are not necessary because these absorbers are optically thick to such radiation. We therefore do not apply a correction for S III. For photons with energies $h\nu < 13.6$ eV, the H I gas is transparent, and thus N(S II) = N(S).

Assuming that DLAs arise in a neutral plus mildly ionized region, Vladilo et al. (2001) model ionization correction terms for sulfur. Depending on the ionization parameter U (the surface flux of ionizing photons divided by the hydrogen particle density), the correction would be in the range $0.15 \geq \log (C[S/H]_I) \geq -0.20$ for $\log N(H) = 20.34$ (their Fig. 9). We consider this range of correction terms as an indication for the size of possible systematic errors in our abundance determination.

Thus, we derive a sulfur abundance of $[S/H]_I = -0.50 \pm 0.33$, or 0.29 solar.

4. ABUNDANCE ANALYSIS: IONIZED GAS

We use [S II] fluxes from region 5 (Schulte-Ladbeck et al. 2004). The rest-frame fluxes are F_{6717} = (0.61 ± 0.09) ×

TABLE 1
COLUMN DENSITIES DERIVED FROM S II LINES

Rest Frame (Å)	Observed (Å)	EW (Å)	REW (Å)	f (cm)	N (10^{15} cm^{-2})
1250.58	1262.54	0.061 ± 0.023	0.060	0.00545	0.80 ± 0.30
1253.81	1265.85	0.173 ± 0.034	0.171	0.01088	1.13 ± 0.23
1259.52	1271.61	0.243 ± 0.050	0.241	0.01624	1.06 ± 0.21

10^{-16} ergs s^{-1} cm^{-2}, $F_{6731} = (0.46 \pm 0.09) \times 10^{-16}$ ergs s^{-1} cm^{-2}, and $F_{H\beta} = (2.13 \pm 0.43) \times 10^{-16}$ ergs s^{-1} cm^{-2}. The electron temperature is $T_e = 11300^{+2100}_{-1500}$ K, and the electron density is $n_e \approx 80$ cm^{-3}.

We use the task IONIC (Shaw & Dufour 1995) to derive abundances from the line-flux measurements. This results in $[\mathrm{S\ II/H}]_{II} = -1.25 \pm 0.30$ for the H II region. Errors are estimated by exploring the effects on the outcome of the model when varying the input values with their errors. As a consistency check, we also calculate the abundance of S II/H by applying equation (11) of Pagel et al. (1992). This gives $[\mathrm{S\ II/H}]_{II} = -1.31 \pm 0.45$. The errors are calculated by error propagation. In the remainder of the text, we will refer to the value derived by using IONIC.

Note that the spectra of Schulte-Ladbeck et al. (2004) do not cover the strong [S III] lines at 9069 and 9532 Å. The weak [S III] line at 6312.06 Å was covered by the William Herschel Telescope ISIS R600R/TEK4 spectrum observed on 2000 April 25. We measure a rest-frame flux of $F_{6312} = (0.11 \pm 0.09) \times 10^{-16}$ ergs s^{-1} cm^{-2} in H II region 5. This leads to $[\mathrm{S\ III/H}]_{II} = -0.32 \pm 0.30$. To estimate the error, we again explored the outcome of IONIC by varying the input values with their errors. Thus, we derive $[\mathrm{S/H}]_{II} = [\mathrm{S\ II + S\ III/H}]_{II} = -0.27 \pm 0.30$ for the total sulfur abundance. We calculate $[\mathrm{S\ III/H}]_{II} = -0.36 \pm 0.40$ using equation (12) of Pagel et al. (1992) as a consistency check, thus $[\mathrm{S/H}]_{II} = -0.31 \pm 0.30$. As another check, we apply a correction factor from photoionization models to the measured S II abundance to account for S III in the H II region. Garnett (1989) intensively studied sulfur in extragalactic H II regions. Typically, one observes two major ionization states: S II and S III. Schulte-Ladbeck et al. (2004) measured $(\mathrm{O\ II/O\ I})_{II} = 0.41$. With this oxygen ratio, we can correct for the unseen S III. Using Figure 4 from Garnett (1989) leads to a correction factor of $\log (\mathrm{S\ II/S\ III})_{II} = -1.0 \pm 0.2$, and we derive $[\mathrm{S/H}]_{II} = -0.21 \pm 0.30$. Whereas S IV becomes important in highly ionized nebulae, or if $(\mathrm{O\ II/O\ I})_{II} < 0.3$, the measured $(\mathrm{O\ II/O\ I})_{II}$ ratio suggests that this ion does not make an important contribution in our case.

5. RESULTS

The measured sulfur column density in the neutral gas, $N(\mathrm{S\ II}) = 1.10 \times 10^{15}$ cm^{-2}, is consistent with the prediction of Schulte-Ladbeck et al. (2004), $N(\mathrm{S\ II}) = 1.15 \times 10^{15}$ cm^{-2}.

They used three methods to determine $[\mathrm{O/H}]_{II} = -0.54 \pm 0.20$. *HST*/Faint Object Spectrograph data revealed $[\mathrm{O/H}]_{I} > -2.14$. Here we find $[\mathrm{S/H}]_{II} = -0.27 \pm 0.30$, and $[\mathrm{S/H}]_{I} = -0.50 \pm 0.33$. Within the errors, these four values are the same. Schulte-Ladbeck et al. (2004) derived $\log (\mathrm{N/O})_{II} = -1.40^{+0.20}_{-0.30}$. Here we calculate a range of $-2.0 \lesssim \log (\mathrm{N/S})_{I} \lesssim -0.8$. Again, we find agreement.

6. DISCUSSION

Figure 3 offers us a comparison between the metallicities ($[\mathrm{O/H}]_{II}$) of local SFGs and the metallicities ($[\mathrm{O, S, Si/H}]_{I}$) of high-redshift DLAs. Synthesized in massive stars, O and Si are both made by α-capture, while S originates from the explosive burning of O (Woosley et al. 2002). Nissen et al. (2004) recently studied S in Galactic halo stars and showed empirically that S behaves like an α-capture element. Thus, we use it as a proxy for O. Note that the gas-phase Si abundances may be slightly underestimated in DLAs since Si depletes onto dust grains.

In the local universe, accurate oxygen abundances are determined using the direct or T_e method. I Zw 18 is the local galaxy with the lowest oxygen abundance on record, -1.56 ± 0.01 (Izotov & Thuan 1999). Even the analysis of a large sample of Sloan Digital Sky Survey (SDSS) spectra using the T_e method (Kniazev et al. 2004) has not turned up a galaxy with a lower oxygen abundance. Neither has a lower abundance been found in the outskirts of local spirals (van Zee et al. 1998). The local H II region with the highest known oxygen abundance, 0.2 ± 0.2, resides in NGC 1232 (Castellanos et al. 2002). These minimum and maximum values are indicated in Figure 3 by dashed lines.

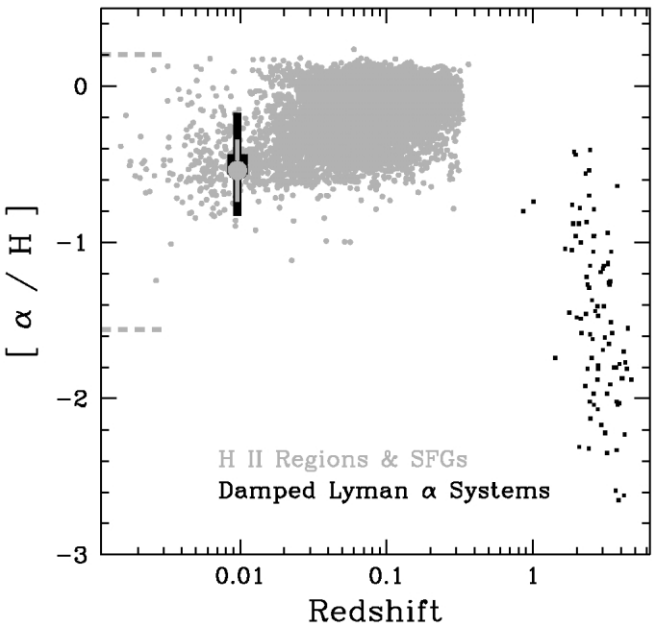

FIG. 3.—Metallicity as a function of redshift. The dashed lines indicate the minimum and maximum local universe values of $[\mathrm{O/H}]_{II}$ (see text). The gray circles are values of $[\mathrm{O/H}]_{II}$ for H II regions and SFGs from the SDSS. The black squares are values of $[\mathrm{O, S, Si/H}]_{I}$ from the compilation of Prochaska et al. (2003a). The neutral ($[\mathrm{S/H}]_{I}$) and ionized ($[\mathrm{O/H}]_{II}$) gas-phase abundances of SBS 1543+593 are overlaid. Their agreement indicates that the metallicities of SFGs and DLAs can be interpreted within the same framework.

To illustrate the oxygen abundances at low redshifts, we plot in Figure 3 oxygen abundances for local H II regions and SFGs from the SDSS, using the selection criteria described in Schulte-Ladbeck et al. (2003) and applying the O3N2 strong-line indices of Pettini & Pagel (2004) after adding 1.3 Å to the rest equivalent widths of Hα and Hβ to account for underlying stellar Balmer absorption (Hopkins et al. 2003). The median error based on line fluxes is 0.05, and following Pettini & Pagel, the systematic errors are 0.14 (their eq. [3]) and 0.18 (their eq. [2]). Our illustrative [O/H] values for the redshift range from 0 to 0.3 span the range from −1.2 to 0.2 and represent well the local T_e-based values. Note that our median metallicities are systematically lower than those derived by Tremonti et al. (2004) for SDSS SFGs; this is presumably due to different methodologies. Adopting their [O/H] ratios would exacerbate the difference between SFG and DLA metallicities.

For the DLAs, we plot in Figure 3 the $[\mathrm{O/H}]_{I}$, $[\mathrm{S/H}]_{I}$, and $[\mathrm{Si/H}]_{I}$ ratios from the compilation of Prochaska et al. (2003a). The median [α/H] error in this sample is 0.1.

Our main observations are the following: $[\mathrm{O, S, Si/H}]_{I}$ of high-redshift DLAs go down to −2.6. Such low metallicities are unobserved in the local universe! DLA metallicities reach as high as $[\mathrm{O, S, Si/H}]_{I} = -0.4$, but never once do they attain the supersolar values observed in local galaxies. Are these two populations at all comparable?

We enter in Figure 3 the values for SBS 1543+593 as follows. For the neutral gas abundance, we show $[\mathrm{S/H}]_{I}$, and for

the ionized gas abundance, we show $[O/H]_{II}$. Here is one DLA for which we can demonstrate that, in principle, emission- and absorption-line techniques give the same results when chemical elements with similar nucleosynthetic origins are compared at similar locations within a DLA galaxy.

There have long been discussions about whether or not emission- and absorption-line diagnostics yield the same chemical abundances in SFGs when one uses the internal star-forming regions rather than a QSO as the background light source for the absorption experiment (e.g., Pettini & Lipman 1995; Pettini et al. 2002; Aloisi et al. 2003; Lecavelier des Etangs et al. 2004). There is as yet no agreement on the issue. A few recent studies have addressed chemical abundances in (sub-)DLAs, but these works do not compare the same elements in absorption and in emission (e.g., Christensen et al. 2005; Ellison et al. 2005; Chen et al. 2005). The case we have here does not suffer from any of these uncertainties. Furthermore, in other DLA galaxies, the QSO intercepts the galaxy's disks at a much larger impact parameter, so internal metallicity gradients have to be accounted for. Therefore, ours is the cleanest comparison made to date between emission- and absorption-line abundances in a DLA/SFG.

The agreement between the metallicity in the neutral gas phase and that in the ionized gas phase of SBS 1543+593 validates, in principle, the comparisons between the two types of objects, SFGs and DLAs, on the metallicity versus redshift diagram. SBS 1543+593 thus makes the case that metal enrichment has taken place in the gas-rich, star-forming galaxy population between redshifts of 5 and 0.

In practice, galaxy metallicity gradients must be important for a detailed comparison between SFG and DLA metallicities. DLAs are merely defined by a neutral H column density threshold, and yet we do not know where a given DLA line is produced within a high-redshift galaxy's disk. Galaxy metallicity gradients have been investigated for local disk galaxies, but it remains to be seen how they behave as a function of redshift. First insights on this issue are provided by the work of Chen et al. (2005).

7. CONCLUSIONS

We investigated the O/H, S/H, and N/O ratios in the ionized gas of the DLA galaxy SBS 1543+593 and compared them with the O/H, S/H, and N/S ratios in its neutral gas. We find that the metallicities in the ionized and neutral gas agree within the errors. The experiment allows us to interpret DLA metallicities as an extension of SFG metallicities to high redshift, suggesting that gas-rich galaxies had lower metallicities at higher redshifts when they were younger.

This Letter is based in part on *HST* archival data. We thank David Bowen for communicating his preliminary [S/H] results while the data were still proprietary. R. E. S.-L. and A. M. H. gratefully acknowledge support awarded by the Space Telescope Science Institute, which is operated by the Association of Universities for Research in Astronomy, Inc., for NASA, under contract NAS 5-26555. Max Pettini and Sandhya Rao are thanked for their useful discussions of the Letter. Please note that Prochaska et al. (2003a) contains a long list of original references that we did not repeat here in the interest of brevity. We acknowledge the use of the SDSS archive.[6] Our work is based on observations (GN-2004A-Q-82) obtained at the Gemini Observatory. We thank Marcel Bergmann for assistance with the Gemini observations.

[6] The SDSS Web site is http://www.sdss.org and lists all partners.

REFERENCES

Aloisi, A., Savaglio, S., Heckman, T. M., Hoopes, C. G., Leitherer, C., & Sembach, K. R. 2003, ApJ, 595, 760
Bowen, D. V., Huchtmeier, W., Brinks, E., Tripp, T. M., & Jenkins, E. B. 2001a, A&A, 372, 820
Bowen, D. V., Tripp, T. M., & Jenkins, E. B. 2001b, AJ, 121, 1456
Castellanos, M., Díaz, A. I., & Terlevich, E. 2002, MNRAS, 329, 315
Chen, H.-W., Kennicutt, R. C., Jr., & Rauch, M. 2005, ApJ, 620, 703
Christensen, L., Schulte-Ladbeck, R. E., Sánchez, S. F., Becker, T., Jahnke, K., Kelz, A., Roth, M. M., & Wisotzki, L. 2005, A&A, 429, 477
Ellison, S. L., Kewley, L. J., & Mallén-Ornelas, G. 2005, MNRAS, 357, 354
Garnett, D. R. 1989, ApJ, 345, 282
———. 2004, in Cosmochemistry: The Melting Pot of the Elements, ed. C. Esteban et al. (Cambridge: Cambridge Univ. Press), 171
Grevesse, N., & Sauval, A. J. 1998, Space Sci. Rev., 85, 161
Holweger, H. 2001, in AIP Conf. Proc. 598, Solar and Galactic Composition: A Joint *SOHO*/*ACE* Workshop, ed. R. F. Wimmer-Schweingruber (Melville: AIP), 23
Hopkins, A. M., et al. 2003, ApJ, 599, 971
Izotov, Y. I., & Thuan, T. X. 1999, ApJ, 511, 639
Kniazev, A. Y., Pustilnik, S. A., Grebel, E. K., Lee, H., & Pramskij, A. G. 2004, ApJS, 153, 429
Lecavelier des Etangs, A., Désert, J.-M., Kunth, D., Vidal-Madjar, A., Callejo, G., Ferlet, R., Hébrard, G., & Lebouteiller, V. 2004, A&A, 413, 131
Morton, D. C. 1991, ApJS, 77, 119
Nissen, P. E., Chen, Y. Q., Asplund, M., & Pettini, M. 2004, A&A, 415, 993
Pagel, B. E. J., Simonson, E. A., Terlevich, R. J., & Edmunds, M. G. 1992, MNRAS, 255, 325
Petitjean, P. 1998, preprint (astro-ph/9810418)
Pettini, M. 2004, in Cosmochemistry: The Melting Pot of the Elements, ed. C. Esteban et al. (Cambridge: Cambridge Univ. Press), 257
Pettini M., & Lipman, K. 1995, A&A, 297, L63
Pettini, M., & Pagel, B. E. J. 2004, MNRAS, 348, L59
Pettini, M., Rix, S. A., Steidel, C. C., Adelberger, K. L., Hunt, M. P., & Shapley, A. E. 2002, ApJ, 569, 742
Prochaska, J. X., Gawiser, E., Wolfe, A. M., Castro, S., & Djorgovski, S. G. 2003a, ApJ, 595, L9
Prochaska, J. X., Gawiser, E., Wolfe, A. M., Cooke, J., & Gelino, D. 2003b, ApJS, 147, 227
Reimers, D., & Hagen, H.-J. 1998, A&A, 329, L25
Schulte-Ladbeck, R. E., Miller, C. J., Hopp, U., Hopkins, A., Nichol, R. C., Voges, W., & Fang, T., 2003, preprint (astro-ph/0312069)
Schulte-Ladbeck, R. E., Rao, S. M., Drozdovsky, I. O., Turnshek, D. A., Nestor, D. B., & Pettini, M. 2004, ApJ, 600, 613
Shaw, R. A., & Dufour, R. J. 1995, PASP, 107, 896
Tremonti, C. A., et al. 2004, ApJ, 613, 898
Turnshek, D. A., Rao, S. M., & Nestor, D. B. 2002, in ASP Conf. Ser. 254, Extragalactic Gas at Low Redshift, ed. J. S. Mulchaey & J. Stocke (San Francisco: ASP), 42
van Zee, L., Salzer, J. J., Haynes, M. P., O'Donoghue, A. A., & Balonek, T. J. 1998, AJ, 116, 2805
Vladilo, G., Centurión, M., Bonifacio, P., & Howk, J. C. 2001, ApJ, 557, 1007
Wolfe, A. M. 1990, in The Interstellar Medium in Galaxies, ed. H. A. Thronson & J. M. Shull (Dordrecht: Kluwer), 387
Woosley, S. E., Heger, A., & Weaver, T. A. 2002, Rev. Mod. Phys., 74, 1015